

Homogeneous isotropic turbulence in dilute polymers

By E. DE ANGELIS,¹ C. M. CASCIOLA,¹
R. BENZI² AND R. PIVA¹

¹Dipartimento di Meccanica e Aeronautica, Università di Roma ‘La Sapienza’, Via Eudossiana
18, 00184 Roma, Italy

²Dipartimento di Fisica e INFM, Università di Roma ‘Tor Vergata’, Via della Ricerca
scientifica 1, 00133 Roma, Italy

(Received 19 January 2005 and in revised form 22 January 2005)

The modification of the turbulent cascade by polymeric additives is addressed by direct numerical simulations of homogeneous isotropic turbulence of a FENE-P fluid. According to the appropriate form of the Kármán–Howarth equation, two kinds of energy fluxes exist, namely the classical transfer term and the coupling with the polymers. Depending on the Deborah number, the response of the flow may result either in a pure damping or in the depletion of the small scales accompanied by increased fluctuations at large scale. The latter behaviour corresponds to an overall reduction of the dissipation rate with respect to an equivalent Newtonian flow with identical fluctuation intensity. The relevance of the position of the crossover scale between the two components of the energy flux with respect to the Taylor microscale of the system is discussed.

1. Introduction

The addition of a tiny amount of polymer in a turbulent flow produces a substantial decrease of drag and this phenomenon is well documented in experiments (Virk 1975). However, despite extensive experimental and theoretical efforts, the drag reduction mechanism (DR) is still under debate (see Sreenivasan & White 2000). Recently, numerical simulations have become an important tool to understand this intriguing phenomenon (Sureshkumar, Beris & Handler 1997; Min, Yoo & Choi 2001; De Angelis, Casciola & Piva 2002*a*; Dimitropoulos *et al.* 2005).

One of the basic questions concerning DR is the effect of polymers on fluxes of energy across scales and on spatial transfer of momentum in a turbulent flow. In boundary layers the two processes occur simultaneously: in the log-region momentum is transferred towards the wall via Reynolds stresses while a cascade of energy through the scales takes place to dissipate turbulent energy. In this respect, the polymers should alter both the cascade and the momentum transfer in order to give rise to an increased buffer region which produces the increased throughput corresponding to DR (Lumley 1973).

In homogeneous and isotropic turbulence there is no mean shear, hence the polymers cannot change the momentum fluxes in the system. However, they can change the energy flux from large to small scales in a way which will be described in the present paper.

Though this fundamental issue is easily addressed numerically, important aspects of the problem were highlighted by considering decaying grid-generated turbulence.

For instance, McComb, Allan & Greated (1977) discuss longitudinal spectra which unequivocally show a significant alteration of the kinetic energy distribution among scales. This suggests a strong modification of the nature of the cascade, which apparently leads to a substantial depletion of the energy content of the small scales. In a similar context, van Doorn, White & Sreenivasan (1999) clearly show how the decay rate of grid-generated turbulence is reduced by the polymers. The presence of polymers gives rise to a dissipation rate smaller than expected for a corresponding Newtonian flow. The same phenomenon, observed in the context of shell models (see Benzi *et al.* 2003) and accompanied by some increase of fluctuation amplitude at large scale, has been interpreted as a form of generalized DR. The possibility offered by shell models of investigating a wide range of parameters led to the conjecture that increased fluctuations may occur when the Taylor scale is smaller than the Lumley scale of the system (Lumley 1973).

We present numerical simulations of viscoelastic homogeneous and isotropic turbulence aimed at understanding how the polymer stretching changes the energy flux and at which characteristic scales these changes are observed (see Casciola *et al.* 2003 for a related approach in Newtonian shear-dominated turbulence). The polymers are described by the FENE-P model which, for turbulent channel flows, reproduces the features observed in laboratory experiments. After a preliminary study two typical cases are discussed to address the behaviour of the system when changing the Lumley scale.

2. The evolution equations for dilute polymer solutions

The momentum balance for a dilute solution of long chain polymers is

$$\frac{\partial u_i}{\partial t} + u_k \frac{\partial u_i}{\partial x_k} = -\frac{\partial p}{\partial x_i} + \nu \frac{\partial^2 u_i}{\partial x_j \partial x_j} + \frac{\partial T_{ij}}{\partial x_j} + f_i, \quad (2.1)$$

where u_i is the solenoidal velocity field, f_i is the external forcing, p is the pressure normalized by the density and ν is the solvent kinematic viscosity, and the extra stress T_{ij} due to the polymers has the following constitutive relation:

$$T_{ij} = (\nu_p/\tau) [P(R_{kk}; \rho_m, \rho_0) R_{ij}/\rho_0^2 - \delta_{ij}]. \quad (2.2)$$

Here ν_p is a constant of the order of a fraction of ν , depending on polymer concentration, ρ_0 and ρ_m are equilibrium and maximum allowed length of the chains respectively. The conformation tensor, R_{ij} , statistically characterizes the behaviour of the polymers and the Peterlin function, $P = (\rho_m^2 - \rho_0^2)/(\rho_m^2 - R_{kk})$, is a dimensionless nonlinear spring coefficient. In the equation for R_{ij} ,

$$\frac{D R_{ij}}{Dt} = \frac{\partial u_i}{\partial x_k} R_{kj} + R_{ik} \frac{\partial u_k}{\partial x_j} - \frac{1}{\tau} (P R_{ij} - \rho_0^2 \delta_{ij}) + \chi \frac{\partial^2 R_{ij}}{\partial x_k \partial x_k}, \quad (2.3)$$

τ is the largest relaxation time of the chains and the Laplacian represents the diffusion of polymers, usually negligible. Here, it has the role of an artificial diffusion (see Sureshkumar *et al.* 1997) needed to stabilize the high-wavenumber instability. The system (2.1)–(2.3), completed with the continuity equation, is the FENE-P model (Finite Extensibility Nonlinear Elastic-Peterlin) for dilute polymers, see e.g. Bird *et al.* (1987).

The extra stress does work on the velocity according to the balance equation

$$\frac{D(u^2/2)}{Dt} = \frac{\partial(p\delta_{ij} + 2\nu e_{ij})u_i}{\partial x_j} + \frac{\partial(T_{ij}u_i)}{\partial x_j} - \epsilon_N - S + f_i u_i, \quad (2.4)$$

where $\epsilon_N = 2\nu e_{ij}e_{ij}$ is the Newtonian component of the dissipation, with e_{ij} the deformation-velocity tensor. The stress power $S = T_{ij}\partial u_i/\partial x_j$ represents energy per unit time that the chains can either dissipate or store as free energy a according to the balance

$$\frac{Da}{Dt} = S - \epsilon_P, \quad (2.5)$$

where the free energy of the polymer ensemble is

$$a = -\frac{1}{2} \frac{\nu_P}{\tau} \left\{ (\rho_{max}^2/\rho_0^2 - 1) \log \left[(\rho_{max}^2 - R_{kk}) / (\rho_{max}^2 - \rho_0^2) \right] + 1/3 \log (\det R/\rho_0^2) \right\}$$

and $\epsilon_P = (\nu_P/2\tau^2) f[(fR/\rho_0^2)_{kk} + (fR/\rho_0^2)_{kk}^{-1} - 6]$ is the positive definite polymeric dissipation. In terms of micromodelling, the polymeric dissipation described by the relaxation term – the third term on the right-hand side of (2.3) – is due to the Stokes friction of the solvent on the beads of the dumbbells taken to model the individual polymeric chains. For the total free energy in the system, $E = u^2/2 + a$, we have

$$\frac{DE}{Dt} = f_i u_i - \epsilon_T + \frac{\partial J_k}{\partial x_k} \quad (2.6)$$

where J_i is the corresponding spatial flux and $\epsilon_T = \epsilon_N + \epsilon_P$. The term S , as a conservative exchange of energy between microstructure and fluid, drops out from (2.6).

3. Global features of the flow

3.1. Forcing mechanism and dimensionless parameters

Equations (2.1), (2.3) have been integrated in a triperiodic domain of length $l_x = 2\pi$ using a Fourier spectral method and a third-order Runge–Kutta time solver with the nonlinear terms de-aliased by the 3/2 rule. A random forcing is applied to the first shell of wave vectors, with amplitude $\hat{f}_0 = 0.2$, constant in time and uniformly distributed phases and directions. The phase is subject to the condition of positive energy injection. As a consequence, the input power may change with the parameters of the flow and the results have to be normalized before comparison. The procedure yields a statistically stationary isotropic field where input power and total dissipation balance. The simulation parameters include the Reynolds number $Re = (l_x^3 \hat{f}_0)^{(1/2)}/\nu_T$, where $U_0 = (l_x \hat{f}_0)^{(1/2)}$ is the external velocity scale and $\nu_T = \nu + \nu_P$, the Deborah number $De = \tau(\hat{f}_0/l_x)^{1/2}$ where $T = (l_x/\hat{f}_0)^{(1/2)}$ is the characteristic time, $\alpha = (\rho_m/\rho_0)^2$ and the viscosity ratio, $\eta_P = \nu_P/\nu$. In all the simulations $Re = 960$, $\alpha = 1000$, $\eta_P = 0.1$. After reaching a statistically steady state, each run has been continued up to time $T_{max} = 550T \simeq 3000$ to collect the amount of data required for well-converged statistics. Each simulation has been repeated twice with the number of nodes increased from 64^3 to 128^3 (96^3 and 192^3 , due to de-aliasing). The finer grid for the polymer case requires a computational effort comparable with a standard 512^3 Newtonian simulation, due to the increase of number of variables, of nonlinear terms for each equation and of integration time.

We discuss two viscoelastic cases at $De = 0.18$ and 0.54 . Typical realizations of the field are shown in figure 1, where, apparently, viscoelasticity leads to structures with increased dimensions. The coherence factors of the velocity, i.e. $\langle u_i u_j \rangle / (\langle u_i^2 \rangle \langle u_j^2 \rangle)^{1/2}$ with $i \neq j$, always below 2%, imply a substantial isotropy of the simulations.

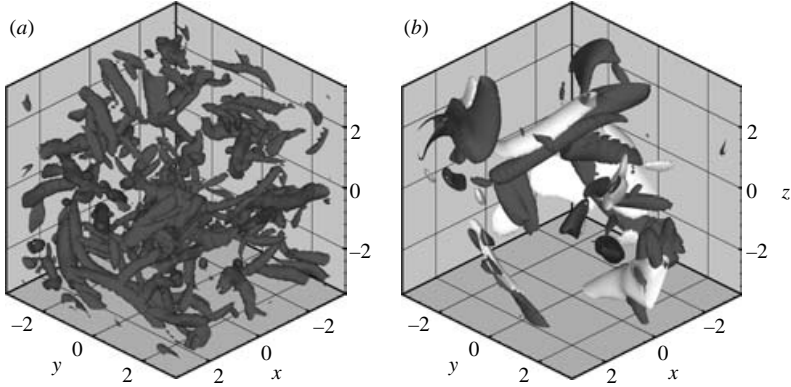


FIGURE 1. Vortical structures (grey) for (a) the Newtonian and (b) the viscoelastic case at $De=0.54$. In (b) an isosurface of 30% of the maximum value of the polymer dissipation ϵ_p is also plotted (white).

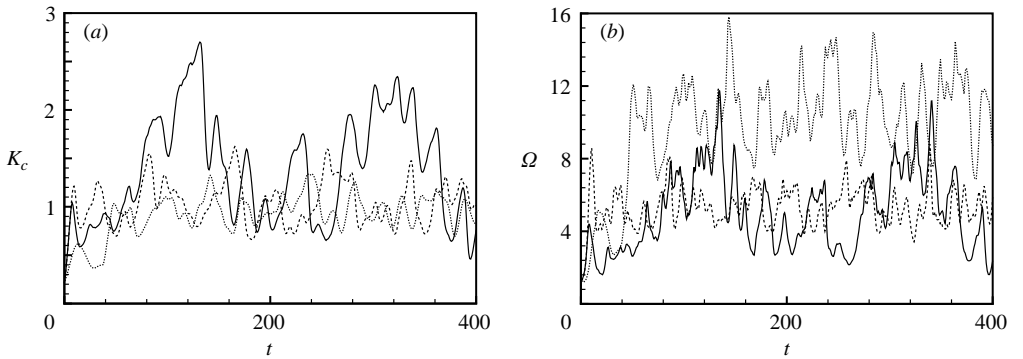


FIGURE 2. (a) A small portion of the time history of the spatial average of the kinetic energy K_c . Dotted, dashed and solid lines correspond to $De=0$, $De=0.18$, and $De=0.54$, respectively. (b) History of the spatial average of Ω in the same time interval, same line styles.

De	u_{rms}	$\bar{\epsilon}_T = \langle f \cdot u \rangle$	D	$\bar{\epsilon}_N$	$\bar{\epsilon}_P$	λ	η	r_e^*	ℓ_p	$\langle R_{kk} \rangle / \rho_0^2$	N_{modes}
0	0.806	0.156	1.87	0.156	—	0.68	0.040	—	—	—	64^3
0.18	0.832	0.174	1.90	0.072	0.102	0.98	0.045	1.23	0.603	154	64^3
0.54	0.989	0.238	1.55	0.070	0.164	1.18	0.045	2.20	0.973	520	64^3
0.54	0.969	0.232	1.60	0.074	0.158	1.14	0.045	2.20	0.923	532	128^3

TABLE 1. Summary of the principal global quantities. For the definitions of r_e^* and ℓ_p see text and equations (4.5) and (4.7), respectively.

3.2. Kinetic energy and large-scale fluctuations

The principal global quantities are reported in table 1, where the most relevant feature is the increase of the kinetic energy $K_c = (3/2)u_{rms}^2$ with De . This effect, illustrated in figure 2(a), indicates that the polymers can alter the energy-containing range of the system. Before going into details, however, we need to define the best way to normalize the fluctuation intensity and to compare the different cases.

It is well known that in Newtonian homogeneous and isotropic turbulence at high Reynolds number the rate of energy dissipation ϵ is independent of the Reynolds

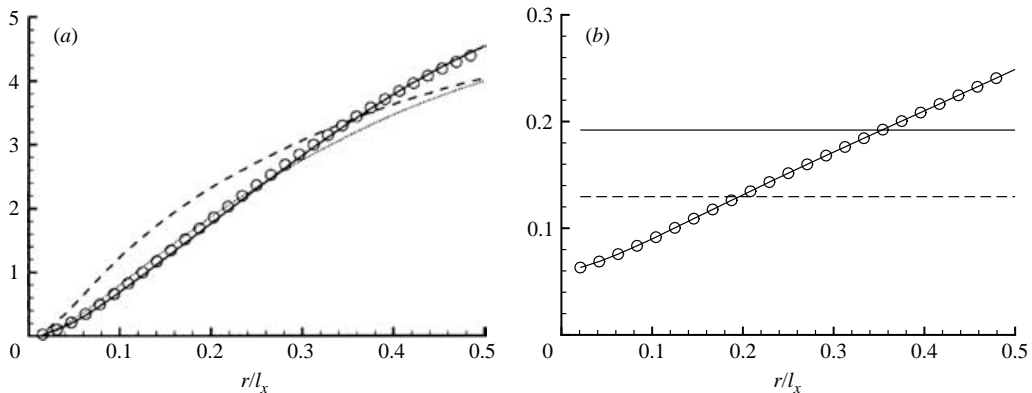


FIGURE 3. (a): $\langle \delta V^2 \rangle / (\bar{\epsilon}_T l_x)^{2/3}$ vs. r/l_x for $De = 0$ (Newtonian) (dashed line), $De = 0.18$ (dotted line) and $De = 0.54$ (solid line and open circles, 64^3 and 128^3 simulation, respectively). (b) Dimensionless eddy turnover time $r / \langle \delta V^2 \rangle^{1/2} \epsilon_T^{1/3} / \ell_x^{2/3}$ for the Newtonian simulation (circles) and effective dimensionless relaxation time $\tau_R \epsilon_T^{1/3} / \ell_x^{2/3}$ for $De = 0.18$ and 0.54 , dashed and solid lines respectively. Crossing of lines and symbols defines the effective Lumley scale, (4.5).

number. For statistically stationary conditions, $\epsilon = D_N u_{rms}^3 / L$ where L is the characteristic scale of the external forcing, i.e. in our case $L = l_x$, and D_N is a dimensionless number, known to be independent of the Reynolds number in Newtonian turbulence, see Sreenivasan (1984). Note that ϵ is also the rate of energy input in the turbulent flow, i.e. $\epsilon = \langle f \cdot u \rangle$. Therefore, the ratio $\epsilon l_x / u_{rms}^3$ represents the energy input ϵ needed in order to produce turbulent fluctuations of intensity u_{rms}^2 . Extending the results to viscoelastic turbulence, the dimensionless dissipation

$$D_P \equiv \langle f \cdot u \rangle l_x / u_{rms}^3 \quad (3.1)$$

is the proper parameter to compare the different cases. When $D_P < D_N$ the overall kinetic energy in the presence of the polymers increases with respect to the Newtonian case. We find (see table 1) that, for $De = 0.54$, $D_P / D_N = 0.85$. The whole picture suggests the alteration of the energy-containing scales of the flow, a most unexpected result for homogeneous isotropic turbulence.

3.3. Enstrophy and small-scale behaviour

Less unexpectedly, the small scales of the system are also strongly affected by polymers, as shown in figure 2(b). However, the enstrophy Ω , as a small-scale quantity, does not exhibit the large cycles which appear in the turbulent kinetic energy. The reduction of the enstrophy with increasing De , i.e. the decrease of the Newtonian dissipation, $\bar{\epsilon}_N = 2\nu \langle \Omega \rangle$, is apparent. On the contrary, the total dissipation, $\bar{\epsilon}_T$, increases, i.e. the flow extracts more power from the constant-amplitude external forcing, as mentioned in §3.1. The fluctuation amplitude also increases, and in certain cases exceeds the input power to obtain the reduction of the dimensionless dissipation rate (3.1).

As shown in table 1, a larger and larger portion of the input power is dissipated by the polymers and, for $De = 0.54$, $\bar{\epsilon}_P$ is 70% of the total. Almost all the energy is contained in the macroscopic kinetic field while most of the dissipation occurs via the polymers. The reduction of $\bar{\epsilon}_N$ leads to the increase of the Kolmogorov length $\eta = (\nu^3 / \bar{\epsilon}_N)^{1/4}$. The Taylor microscale $\lambda = (5 \langle K_c \rangle / \langle \Omega \rangle)^{1/2}$ also increases.

Figure 3(a) shows the second-order structure function $S_2 = \langle \delta V^2 \rangle = \langle \delta V_i \delta V_i \rangle$, where $\delta V_i = u_i(x'_s) - u_i(x_s)$ and $x'_s - x_s = r_s$. In both viscoelastic simulations the polymers affect

the fluctuation intensity at all scales. The detailed picture is however different. For $De=0.18$ the viscoelastic effect amounts to the damping of the fluctuation level and the net result is increased dissipation. At $De=0.54$, the behaviour is more selective. The depletion is confined to the small scales and the fluctuations increase at large scales. The second behaviour is associated with the reduction of D_p , which, on the contrary, slightly increases in the first case.

4. Scale by scale budget

4.1. The Kármán–Howarth equation

In our system the external forcing acts only on the macroscopic field, while both macroscopic flow and the microstructure contribute to the dissipation. The extra stress captures mechanical energy to feed the fluctuations of the microstructure and the associated dissipation. This process affects the flow at all scales.

In order to clarify this alteration and the role of the Deborah number, we address the scale by scale budget of the velocity fluctuations. Starting from the equation for the correlation tensor, $C_{i,j} = \langle u_i u_j \rangle$ where $u'_i = u_i(x'_i)$ and $x'_i - x_i = r_i$, we obtain for a statistically stationary, solenoidal velocity field the Kármán–Howarth equation for the increments, $\delta V_i = u_i(x'_r) - u_i(x_r)$, $\delta V^2 = \delta V_i \delta V_i$, as

$$\frac{\partial}{\partial r_k} \langle \delta V^2 \delta V_k + 2T_{ki}^* \delta V_i \rangle = -4 \langle f_i u_i \rangle + 2 \langle \delta V_i \delta f_i \rangle + 2\nu \frac{\partial^2}{\partial r_k \partial r_k} \langle \delta V^2 \rangle, \quad (4.1)$$

with $T_{ki}^* = T'_{ki} + T_{ki}$. After integrating over a ball B_r of radius r , considering that $\langle f_i u_i \rangle = \bar{\epsilon}_T$, it follows that

$$\begin{aligned} & \frac{1}{4\pi r^2} \oint_{\partial B_r} \langle \delta V^2 \delta V_k + 2T_{ki}^* \delta V_i \rangle n_k \, dS_r \\ &= -(4/3) \bar{\epsilon}_T r + \frac{\nu}{2\pi r^2} \frac{d}{dr} \oint_{\partial B_r} \langle \delta V^2 \rangle \, dS_r + \frac{1}{2\pi r^2} \int_{B_r} \langle \delta V_i \delta f_i \rangle \, dV_r, \end{aligned} \quad (4.2)$$

where the required manipulations do not make use of isotropy but rely heavily on homogeneity (see e.g. Casciola *et al.* 2003 for a similar approach).

The Kármán–Howarth equation (4.2) highlights the main difference between Newtonian and viscoelastic turbulence. For either case, where the viscosity and the correlation $\langle \delta V_i \delta f_i \rangle$ are negligible, the energy flux up to scale r equals the total dissipation. For Newtonian fluids, all the dissipation is provided by the viscosity and the flux is only due to the classical nonlinearity associated with the advection. For viscoelastic fluids, an additional dissipative process takes place in the polymers, and the flux presents a new component which corresponds to the energy intercepted by the microstructure.

4.2. The Yaglom equation for the free energy

For the scale by scale budget we also need an equation for the microstructure. Let us denote by $\psi = S - \epsilon_p$ the excess power, i.e. the power transferred to the polymers in excess of dissipation, which gives the rate of energy storage in the polymers. From (2.5) we can derive the equation for the correlation $\langle aa' \rangle$. Since $\langle a\psi' + a'\psi \rangle = 2\langle a\psi \rangle - \langle \delta a \delta \psi \rangle$ and for a stationary state, $\langle a\psi \rangle = 0$, it can be recast into the form $\partial/\partial r_k \langle \delta V_k \delta a^2 \rangle = 2\langle \delta a \delta \psi \rangle$. After introducing the notation

$$\Psi_S = \frac{2}{4\pi r^2} \int_{B_r} \langle \delta a \delta S \rangle \, dV_r, \quad \Psi_{\epsilon_p} = \frac{2}{4\pi r^2} \int_{B_r} \langle \delta a \delta \epsilon_p \rangle \, dV_r, \quad (4.3)$$

integration over the sphere of radius r yields

$$\frac{1}{4\pi r^2} \oint_{\partial B_r} \langle \delta a^2 \delta V_k \rangle n_k dS_r = \Psi_S - \Psi_{\epsilon_p}. \quad (4.4)$$

Equation (4.4) is the Yaglom-like equation for polymers, which states that the flux of free energy through the spatial scales, i.e. the left-hand side of (4.4), equals the integral of the correlation between fluctuations of free energy, δa , and those of the excess of power, $\delta \psi$. In other words, if an imbalance between fluctuations of S and ϵ_p occurs, it is likely to produce a flux of free energy through the scales of the microstructure.

4.3. Data analysis

As first suggested by Lumley (1973), a relevant scale for the system, r^* , is identified as the scale below which the polymers begin to feel the turbulent fluctuations. It is defined through a time criterion, i.e. comparing the scale-dependent eddy turnover time with the relevant polymer relaxation time. The former is provided by the Newtonian DNS, where as characteristic time for the scale r we assume $r/\langle \delta V^2 \rangle^{1/2}$. The latter is evaluated as $\tau_R = \tau/\langle P \rangle$, since the relaxation time always enters the FENE-P model in its effective form τ/P . As shown in table 1, the polymers are considerably stretched by the turbulence; typically their elongation, $\langle R_{kk} \rangle^{1/2}/\rho_0$, is 70% of the maximum allowed for the case with $De = 0.54$. This implies that $1/P$ may differ considerably from one. The time criterion, figure 3(b), defines the effective Lumley scale by the condition

$$r_e^* / [\langle \delta V_N^2 \rangle (r_e^*)]^{1/2} = \tau_R. \quad (4.5)$$

As shown by table 1, for $De = 0.18$, r_e^* is comparable with the Taylor scale λ , i.e. the polymers act at scales where the inertial dynamics is already affected by viscosity. The overall effect is an increased global dissipation. On the contrary, at $De = 0.54$ r_e^* is substantially larger than λ and the polymers drain energy at inertial scales. This seems to confirm the conjecture of Benzi *et al.* (2003) and explains the effect of polymers on the energy-containing range.

To understand how the polymers modify the energy transfer across scales let us address the Kármán–Howarth equation (4.2). Its left-hand side can be split into the ‘classical part’ due to the convective terms and the viscoelastic contribution given by

$$\Phi_c = \frac{1}{4\pi r^2} \oint_{\partial B_r} \langle \delta V^2 \delta V_k \rangle n_k dS_r, \quad \Phi_p = \frac{1}{4\pi r^2} \oint_{\partial B_r} \langle T_{ki}^* \delta V_i \rangle n_k dS_r, \quad (4.6)$$

respectively, see figure 4(a–c). At large scales, Φ_c contributes most of the energy flux. At small scales the viscoelastic component takes over, entailing the reduction of Φ_c . A crossover scale ℓ_p is clearly identified according to the equation

$$\Phi_p(\ell_p) = \Phi_c(\ell_p). \quad (4.7)$$

The crossover moves towards smaller scales as De is decreased while at the same time the effect of the polymers on the turbulence is reduced. By inspection of the figures, we find that, at the present values of the Reynolds number, the polymers reaction is dynamically relevant in all the available range of scales. Nonetheless, the large scales are less and less affected for decreasing De . Since the Lumley scale delimits the range where polymers feel the turbulence, ℓ_p is generally smaller than r_e^* . Both the scales behave similarly with respect to changes in the Deborah number, see table 1.

Figure 4(d) addresses the Yaglom-like equation for the free energy a . The plots correspond to the two terms of the right-hand side of (4.4), namely Ψ_S due to the stress power and the term due to the dissipation. $\Psi_S - \Psi_{\epsilon_p}$ is always very small,

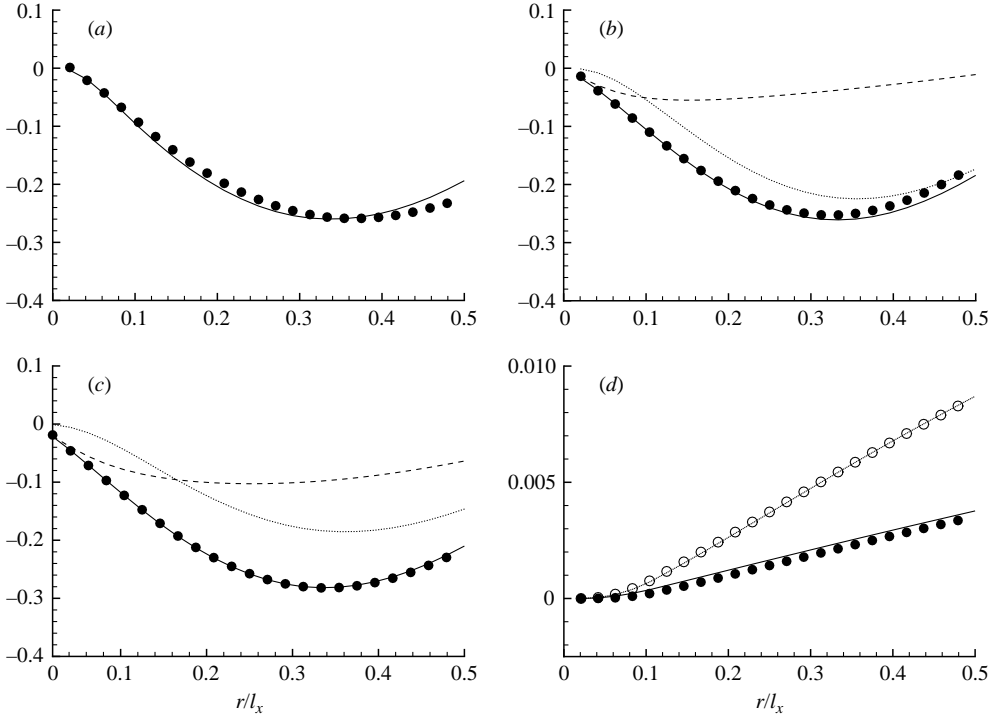


FIGURE 4. Scale by scale budget for (a) the Newtonian, and (b) viscoelastic case at $De=0.18$, and (c) $De=0.54$. The solid line corresponds to $(\Phi_c + \Phi_p)/(\bar{\epsilon}_T l_x)$, with $\Phi_p=0$ in (a). The normalized right-hand side of (4.2) is shown by the symbols. The dashed and dotted lines in (b) and (c) are $\Phi_p/(\bar{\epsilon}_T l_x)$ and $\Phi_c/(\bar{\epsilon}_T l_x)$, respectively. (d) Compares the two contributions to the right-hand side of (4.4), namely Ψ_S (circles) and Ψ_{ep} (lines) for $De=0.18$ and $De=0.54$ (filled and open symbols respectively).

implying that the flux of a , described by the left-hand side of (4.4), is negligible. In other words the fluctuations of stress power are almost immediately converted into fluctuations of polymeric dissipation and no net flux of free energy occurs. This is reasonable for the present cases. Well above r_e^* , the time scale of the fluctuations is larger than the relaxation time, implying that the polymeric dissipation is faster than convection. On the contrary, in the range below r_e^* , i.e. in the proximity of ℓ_p , one should have in principle much faster convective scales. Here, however, the depletion of the velocity fluctuation (see figure 3) explains why polymeric dissipation is still dominant over free-energy transfer.

4.4. Grid sensitivity and artificial diffusion

Grid sensitivity tests have been performed, halving the value of the artificial diffusion coefficient χ when doubling the resolution. The stringent criterion used to select the value of the artificial diffusion coefficient – namely $Sc = \nu/\chi = 0.25$ and 0.5 , for the coarse and the fine grid, respectively – is based on the requirement that the conformation tensor should remain positive definite at every node of the grid for the entire simulation.

The scale-by-scale balance, i.e. the Kármán–Howarth equation of §4.1 and the Yaglom-like equation of §4.2, is virtually unaffected by grid refinement and the related reduction of artificial diffusivity as shown by figure 5. The behaviour of $\langle \delta V^2 \rangle$

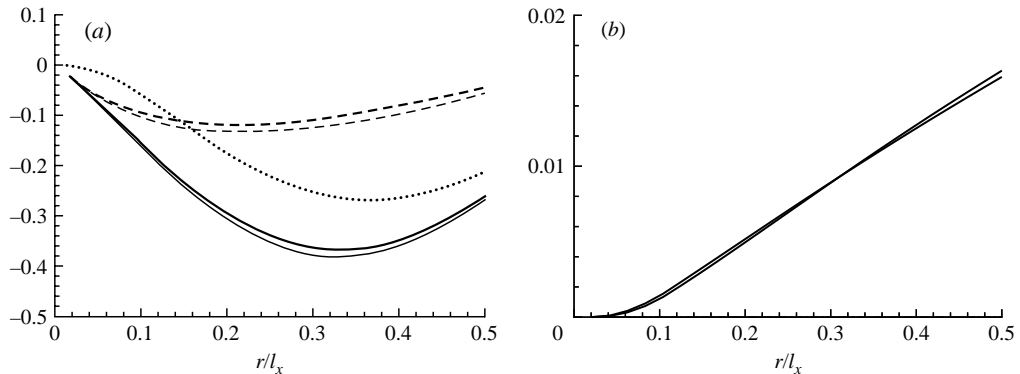


FIGURE 5. Grid sensitivity test at $De = 0.54$. (a) $\Phi_c + \Phi_p$ (solid lines), Φ_p (dashed) and Φ_c (dotted). (b) Ψ_S . Thin and thick lines represent the 64^3 and 128^3 simulations.

is also stable, see the solid line and the open circles in figure 3(a). Neither the crossover scale ℓ_p nor the effective Lumley length r_e^* changes appreciably by doubling the resolution – from table 1 the variation of the first scale is about 3% while the other is unchanged.

Physical considerations lead to the conclusion that the artificial diffusion term, negligible at large scales, becomes effective below a certain scale ℓ_{ad} whose order of magnitude can be estimated by comparison with the relaxation term,

$$\ell_{ad} = \sqrt{\chi\tau/\langle P \rangle}. \quad (4.8)$$

Below ℓ_{ad} , the dynamics may be modified by the artificial term. This scale should be kept well below the scale ℓ_p which characterizes the dynamics of the polymers. For $De = 0.54$, where $\ell_p = 0.97$, $\ell_{ad} = 0.2$ and 0.14 , for the coarse and the fine grid, respectively. We conclude that the discussed depletion of the classical inertial flux in favour of the flux towards the microstructure is physically unaffected by the artificial diffusion.

5. Concluding remarks

Homogeneous isotropic conditions, as achieved here by DNS in triply periodic domains, are ideal for clarifying the issue of the energy cascade in turbulent flows with dilute polymers. According to the Kármán–Howarth equation (§4.1 and De Angelis *et al.* 2002b), the polymers introduce a new component in the energy flux. An alteration of the cascade may result either in a pure damping of the entire range of scales, as for small Deborah numbers, or in the depletion of the small scales accompanied by increased fluctuations at large scales, as for larger values of De . The polymer-induced component of the flux, sub-dominant at large scales, takes over at small scales. When the crossover scale is larger than the Taylor microscale, the flux, from being inertia-dominated, becomes controlled by viscoelasticity. In these conditions an increased turbulence intensity may be observed.

The additional flux of energy always drains energy from the macroscopic kinetic field, i.e. the equivalent effective viscosity is positive at all scales, but the effect is particularly significant near the crossover scale. Consistently, we find that, for the conditions we have investigated, the polymers never give back a net amount of energy to the velocity field. The Yaglom equation for the free energy confirms this conclusion by showing that the scale by scale feeding of the microstructure is dissipated locally in the space of scales.

Finally, we expect the modifications to the cascade to be crucial also in the context of wall bounded flows. For instance, in Sreenivasan & White (2000), revisiting the theory of Tabor & De Gennes (1986), it is argued that the viscoelastic forces at small scales could obstruct the usual Richardson cascade. The cascade would then be terminated at a scale larger than the Kolmogorov length. This could in principle explain the general increase of scales, e.g. buffer layer thickness, which is crucial to understand drag reduction. According to our results, more than obstructed, the classical cascade is ‘intercepted’ by the polymeric component of the energy flux. In a different context, a phenomenological model (L’vov *et al.* 2004) in terms of a space dependent effective viscosity shows that drag reduction follows from the combined effect of Reynolds stress depletion and viscoelastic dissipation. In the light of the present findings, the required increase of effective viscosity must be physically understood as generated by the alteration of the energy cascade we have described here.

In conclusion, the polymers deeply alter the cascade and, at finite Reynolds number, for certain values of relaxation parameter the net dissipation rate is reduced for a given fluctuation level. This point could be important in understanding the effects of polymers on turbulence in general. Clearly the structure of turbulence near the wall is substantially different from the isotropic case considered here. However we are confident that the present approach can be straightforwardly generalized to deal with the wall region.

REFERENCES

- BENZI, R., DE ANGELIS, E., GOVINDARAJAN, R. & PROCACCIA, I. 2003 Shell model for drag reduction with polymer additive in homogeneous turbulence. *Phys. Rev. E* **68**, 016308.
- BIRD, R. B., CURTISS, C. F., ARMSTRONG, R. C. & HASSAGER, O. 1987 *Dynamics of Polymeric Liquids, vol. II Kinetic Theory*. Wiley-Interscience.
- CASCIOLA, C. M., GUALTIERI, P., BENZI, R. & PIVA, R. 2003 Scale by scale budget and similarity laws for shear turbulence. *J. Fluid Mech.* **476**, 105–114.
- DE ANGELIS, E., CASCIOLA, C. M. & PIVA, R. 2002a DNS of wall turbulence: dilute polymers and self-sustaining mechanisms. *Computers Fluids* **31**, 495–507.
- DE ANGELIS, E., CASCIOLA, C. M., BENZI, R. & PIVA, R. 2002b Homogeneous isotropic turbulence in dilute polymers: scale by scale budget. *Chaosdyn-nlin* 0208016.
- DIMITROPOULOS C. D., DUBIEF Y., SHAQFEH E. G., MOIN P. & LELE S. K. 2005 Direct numerical simulation of polymer-induced drag reduction in turbulent boundary layer flow. *Phys. Fluids* **17**, 011705.
- VAN DOORN, E., WHITE, C. M. & SREENIVASAN, K. R. 1999 The decay of grid turbulence in polymer and surfactant solutions. *Phys. Fluids* **11**, 2387.
- L’VOV V. S., POMIALOV, A., PROCACCIA, I. & TIBERKEVICH, V. 2003 Drag reduction by polymers in wall bounded turbulence. *Phys. Rev. Lett.* **92**, 244503.
- LUMLEY, J. L. 1973 Drag reduction in turbulent flow by polymer additives. *J. Polymer Sci., Macrom. Rev.* **7**, 263–290.
- MIN, T., YOO, J. Y. & CHOI, H. 2001 Effect of spatial discretization schemes on numerical solutions of viscoelastic fluid flows. *J Non-Newtonian Fluid Mech.* **100**, 24–47.
- MCCOMB, W. D., ALLAN, J. & GREATED, C. A. 1977 Effect of polymer additives on the small-scale structure of grid-generated turbulence. *Phys. Fluids* **20**, 873–879.
- SREENIVASAN, K. R. 1984 On the scaling of turbulence energy dissipation rate. *Phys. Fluids* **27**, 1048–1051.
- SREENIVASAN, K. R. & WHITE, C. M. 2000 The onset of drag reduction by dilute polymer additives, and the maximum drag reduction asymptote. *J. Fluid Mech.* **409**, 149–164.
- SURESHKUMAR, R., BERIS, A. N. & HANDLER, A. H. 1997 Direct numerical simulation of the turbulent channel flow of a polymer solution. *Phys. Fluids* **9**, 743–755.
- TABOR, M. & DE GENNES, P. G. 1987 A cascade theory of drag reduction. *Europhys. Lett.* **2**, 519–522.
- VIK, P. S. 1975 Drag reduction fundamentals. *AIChE J.* **21**, 625–656.